The Abdus Salam
International Centre for Theoretical Physics

United Nations
Educational, Scientific and
Cultural Organization

IAEA
International Atomic Energy Agency

2055-9

Joint ICTP/IAEA School on Physics and Technology of Fast Reactors Systems

9 - 20 November 2009

Fast Reactor Core Design

Module 3 : Core Thermal Hydraulics

P. Puthiyavinayagam
IGCAR
Kalpakkam
India

IAEA/ICTP School on Physics and Technology of Fast Reactor Systems

Lectures on Fast Reactor Core Design

Module 3 : Core Thermal Hydraulics

Compiled & Delivered by

P,Puthiyavinayagam
IGCAR, Kalpakkam, India

The Abdus Salam
International Centre for Theoretical Physics
Trieste, Italy

Nov 9-20, 2009

3.0 INTRODUCTION

The primary objectives of thermal- hydraulic design of the core are to ensure that adequate flow of coolant is passed through each subassembly (SA) and to determine the temperature and coolant velocity distributions in the core, which are inputs for checking the structural integrity of core components, viz. fuel pin integrity, SA bowing analysis, clad damage etc. The thermal-hydraulic design of core is important in respecting temperature limits while achieving higher mixed-mean outlet temperature.

The important aspects in the thermal hydraulic design of core are as follows.

i) Flow zoning

ii) Temperature distribution in core and subassemblies

iii) Hydraulic aspects of fuel assembly, such as pressure drop, flow regulating devices, hydraulic lifting

iv) Inter and Intra assembly heat transfer

v) Thermal analysis of fuel pin including hot spot analysis

vi) Subassembly flow blockage analysis towards safety

Core thermal hydraulic design is essentially an exercise of optimizing the different design parameters. While the thermal hydraulic design should aim to achieve as high a coolant outlet temperature as possible, it should also satisfy the design safety limits and it should be achieved with the minimum possible primary pump capacity.

3.1 DESIGN CRITERIA

- Design Safety Limits of fuel, clad and coolant are respected during all operational states
- Fuel pin integrity shall be ensured for their life time
- Core subassemblies and pin deformation shall be within their design limits from operational and safety considerations
- Subassemblies shall not get lifted
- Flow blockage in SA shall be avoided
- Wrong loading of subassemblies shall be prevented by design
- Mixed mean coolant temp rise shall be as per the design intent (150 ºC in PFBR)
- There shall not be any cavitation even at 110% of rated flow.
- Temperature difference between two neighbouring SA shall be within 100 ^{o}C (for PFBR) during its life- time from thermal striping consideration
- Hotspot Temperature of fuel, blanket and absorber materials shall be less than the respective melting points with desired margin (115% over power margin in PFBR).
- Coolant velocities should be limited – to prevent cavitation at 110% of rated flow & Flow Induced Vibration and corrosion are within acceptable limits
- Hydraulic Lifting force should be less than the downward force
- Adequate cooling in internal storage positions under all conditions
- Coolant flow zoning to be made in a such way to achieve max average temperature rise by satisfying the various temperature limits

3.2 POWER GENERATION & FLOW ALLOCATION

Coolant flow allocation is based on power generation. Power generation in the core varies due to variation in the flux. Power generation in the different regions of the core for a typical fast reactor having a radial breeder zone is given below:

Region	% of Power
Fuel	85-95
Blanket	8-10
Absorber Rod	0.3-0.5
Shielding	0.1-0.2

The blanket power increases with the burnup due to accumulation of fissile material while the fuel power decreases. This causes a change of radial power profile from beginning-of-life (BOL) to end-of-life (EOL)

As the power distribution in the reactor is not uniform, flow through each SA has to be allocated such that temperature at the outlet of the SA are nearly uniform. However, it is cumbersome to allocate flow for each SA and hence SA having similar powers are grouped together and are assigned the same flow. Given the total power and the temperature rise in the reactor, the total flow through the core gets fixed and this flow is to be distributed through various regions such that the design criteria are met under operating conditions of individual SA. While allocating the flow through each SA, it is necessary to take into account the mixing in the SA as this factor improves the SA average temperature. Also, for blanket SA (BSA), where coolant flow rate is less compared to Fuel SA (FSA), inter SA heat transfer plays an important role. Hence, unless these factors are considered while allocating the flow, flow through the SA will be over predicted. Hence, a judicious estimate of these factors is necessary.

3.3 THERMAL HYDRAULIC ANALYSIS

Thermal-Hydraulic analysis of reactor core is normally performed in three steps.

- Coolant flow distribution in the core (flow zoning)
- Flow and coolant temperature distribution over subassembly cross section
- Temperature distribution in the pins.

for which the following are the input data that would be required.

- Geometry
- Power distribution
- Flow rate
- Coolant and structure properties

SA and pin deformation depend on temperature distribution which in turn depends on the SA & pin geometry and their deformation behaviour and hence it becomes a conjugate problem of core deformation and power distribution.

The following flow chart in Fig. 3.1 shows the thermal hydraulic analysis of a typical fast reactor core.

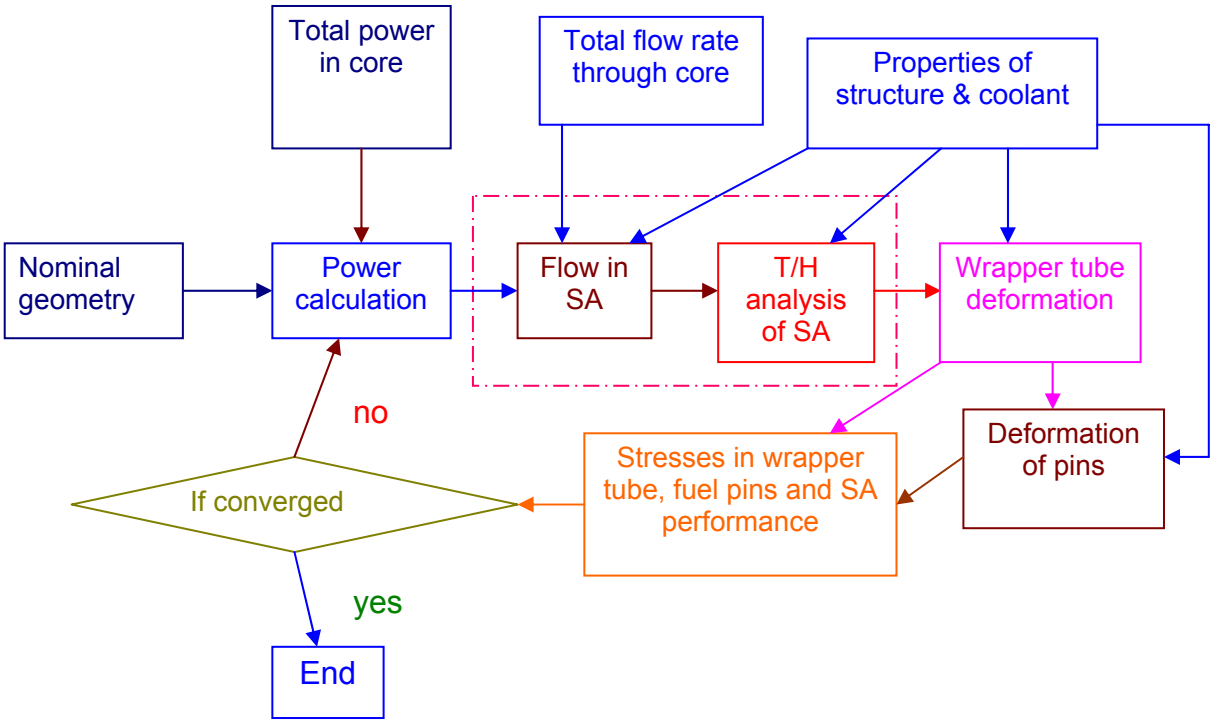

Fig. 3.1 : Thermal hydraulic analysis flow chart

3.4 FLOW ZONING

Due to variation in the flux profile in radial direction, the power profile changes according to the location of the SA on the grid plate and also the power generated in the fuel SA changes from beginning-of-life to end-of-life. Again the blanket power increases with the burnup due to accumulation of fissile material. So, each SA may require different flow to exactly satisfy the temperature limits in all the design basis events. Since all the SAs are in parallel paths, pressure drop devices are fixed at the foot of the SA to regulate the flow. Devising many pressure drop configurations to suit different SA is tedious process and it may lead to fuel handling complications and mechanical interlocks to avoid wrong loading of SAs. So, a zone of SAs whose flow requirement values are closer can be grouped based on the maximum flow requirement of the SA in that group. Due to this fact, the remaining SA in the group receives more flow than the required. The objective of the flow zoning is to maximize the coolant outlet temperature and to minimize the temperature difference between the neighbouring SAs from thermal striping point of view with the constraints of temperature limits of clad, coolant & fuel. It is better to have minimum number of flow zones with the above objective for practical considerations.

Analysis is to be carried out for the flow distribution, preferably a core sector representing symmetry. Flow optimization is to be carried out such that the design

criteria are satisfied. A factor for taking into account the mixing characteristics within a SA and inter SA heat transfer due to the presence of adjacent SA is to be obtained for each SA either by experimental means or by computer codes. While allocating flow, a minimum flow should be allocated to SA in storage locations commensurate with the decay heat from these SA.

For the reactor core containing various types of SA with different power generation, number of flow zones is to be optimized. For a typical core, the optimization is shown in Table 3.1. With increasing number of flow zones, required overall reactor flow comes down.

Based on the flow optimization and rationalization, SA with forced cooling are to be divided into a number of flow zones (In PFBR, there are 15 flow zones. Fuel region is divided into 7 zones, blanket into 3 zones, the control, reflector and shielding having 1 zone each and internal storage locations into 2 zones (1 for spent fuel SA and 1 for failed fuel SA). The necessary flow through SA is realized by providing flow control device like an orifice at the foot of each SA. A typical flow zoning in fuel, blanket & control rod region is shown in Fig. 3.2. The power distribution and flow for a 30^{o} core sector are shown in Fig.3.3. Temperature rise across the hottest channel and SA are shown in Fig.3.4. The clad midwall hotspot and nominal temperatures are shown in Fig.3.5. The values are for a typical fast reactor.

Table- 3.1 Flow zoning Optimisation

Total no. of flow zones	No. of flow zones in each region						Min. required flow rate to meet design criteria (kg/s)
	Fuel Inner	Fuel Outer	Blanket	Control	Reflector & Inner B4C Shielding	Storage	
8	1	2	1	1	1	1	7346.5
9	2	2	1	1	1	1	7059.1
10	2	3	1	1	1	1	6819.9
11	3	3	1	1	1	1	6628.2
12	3	4	1	1	1	1	6547.8
13	3	4	2	1	1	1	6484.8
14	3	4	3	1	1	1	6428.3

Once flow zoning is completed, temperature rise across all core SA can be computed. Then, overall core average outlet temperature can also be computed subsequently. Individual SA outlet temp, both average and max can be computed by SA thermal hydraulic analysis codes. Then, individual fuel pin is analysed to get the clad midwall nominal and hotspot temperatures.

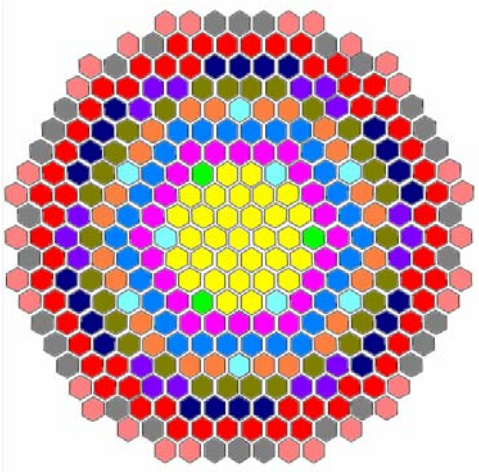

Subassembly	Zone No.	Name	No. of SA in the zone
	1	Fuel inner	31
	2	Fuel inner	24
	3	Fuel inner	30
	4	Fuel outer	24
	5	Fuel outer	30
	6	Fuel outer	18
	7	Fuel outer	24
	8	Blanket	60
	9	Blanket	30
	10	Blanket	30
	11	CSR/DSR	12

Fig. 3.2 : Flow Zoning in typical Fast Reactor Core

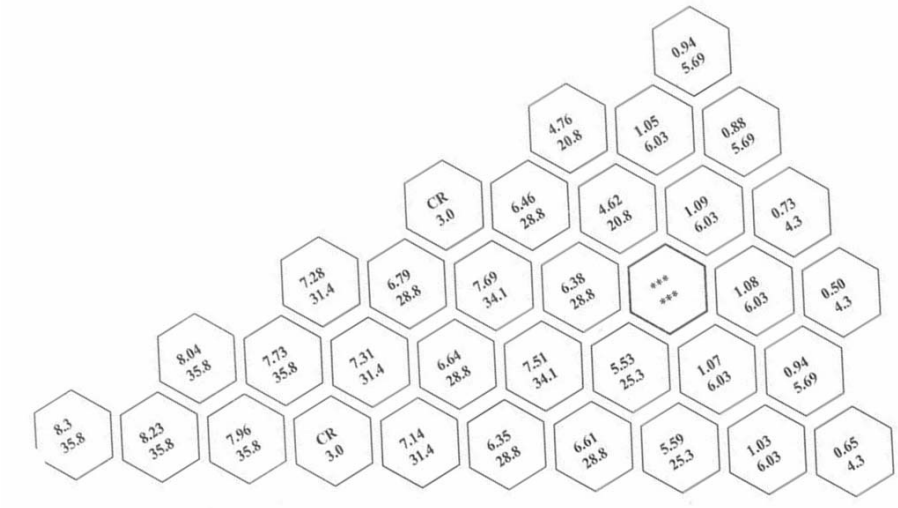

Fig. 3.3: SA power and coolant mass flow rate

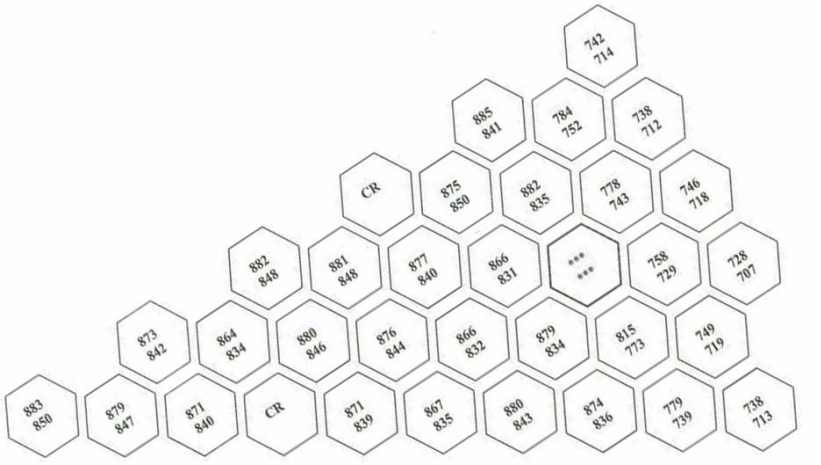

Fig. 3.4: Coolant outlet temp from hottest channel and average SA outlet temp

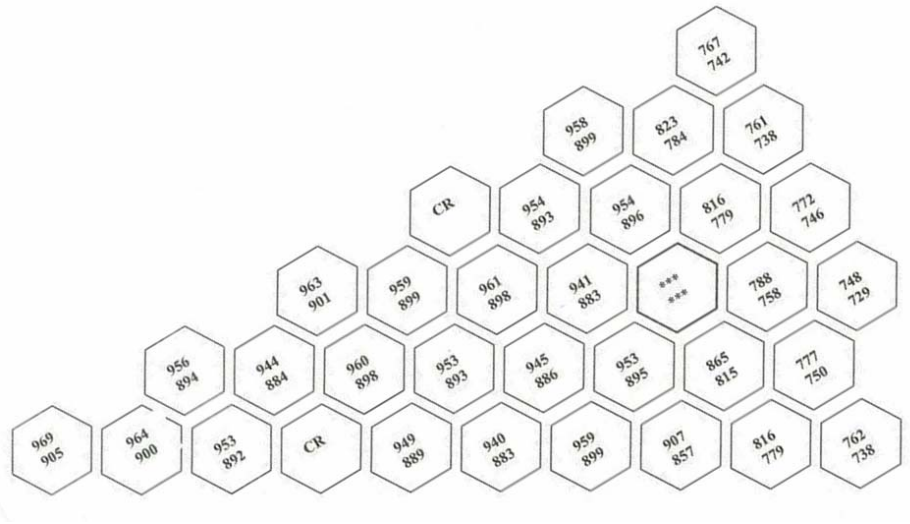

Fig. 3.5 : Clad midwall hotspot and nominal tempeartures

3.5 CORE THERMAL ANALYSIS

After determining the flow rate through each SA, steady-state temperature distribution in a SA is to be determined using multi-assembly codes such as SUPERENERGY. In this code intra- assembly thermal hydraulic behaviour due to the presence of wire wrap around the pins is described in terms of two-correlated parameters, eddy diffusivity (ε^*) and swirl ratio (C). These parameters coupled with numerical form of energy equations and along with a flow split model provide a complete representation of the temperature under forced convection regime. The code should take into account the inter SA heat transfer between the SA which is important for peripheral SA especially for BSA. The analysis is to be made for core symmetric sector involving fuel, blanket and control SA and for the selected coolant inlet temperature. The coolant and clad temperature distribution at the top of the pin-bundle for fuel and blanket SA and also through the axial levels will form the output. Once the coolant temperatures are found out, the pin temperatures are predicted using analytical models at the beginning of life.

3.5.1 Analytical Model

At no point, temperature should exceed the prescribed limit taking into account the uncertainties in predicting the operating temperature of the reactor such as flux pattern, power level, flow distribution etc. Temperature limits are imposed on clad temperatures of fuel, blanket and absorber pins [typical limit for clad mid-wall hot spot temperature for fuel pin is 973 K (700^{o}C)].

Two things that are necessary for the analysis are:

- Development of analytical model and
- Identification of physical parameter & knowledge of change in values of these parameters in the core.

Fuel undergoes restructuring in pile due to temperature and is subjected to fission products swelling, high temperature gradients, fuel-clad interaction at high burn up etc.

At the beginning of life under high temperature condition, analytical model is simple, since the fuel is as fabricated with a gap from clad. However, as the fuel material burns-up, restructuring of fuel takes place.

Considering the fuel as a heat generating ceramic cylinder, we can derive the temperature profile from the one dimensional heat conduction equation:

$$\frac{d^2T}{dr^2} + \frac{1}{r}\frac{dT}{dr} = -\frac{Q}{K}$$

Boundary conditions:

$$\frac{dT}{dr} = 0 \ \ at \ \ r = 0$$

$T = T_s$ at $r = R_f$

Where,
R_f - radius of the fuel
T_S – Fuel surface temperature

Q- Volumetric heat generation in the fuel

Integrating and eliminating the integral constants,

$$\int_{Ts}^{T(r)} KdT = \frac{Q}{4}\left(R_f^2 - r^2\right)$$

The temperature profile from the centreline to the bulk coolant must be arrived at by solving the heat conduction equations with appropriate boundary conditions. One must use this approach for carbide fuel or an un-restructured fuel. When a cylindrical fuel element is placed in a neutron flux, the volumetric heat generation from the resulting fission gives rise to a temperature difference between the centreline and the external surface through which the heat is extracted. This temperature difference, for oxide fuels, is in excess of 10^3 K and since the typical radius of such elements is a few millimetres, average thermal gradients > 10^5 K/m exist. This gradient causes the fuel microstructure to change quite rapidly after the reactor power has been raised to its operating level. So in the case of restructured fuel, a multi zone model with varying densities must be adopted to arrive at the temperature profile across the fuel pellet.

Computer codes use empirical formulae derived from experimental data. For preliminary analysis, normally a singular three density region model is used.

Outer region is the one having as fabricated density (at temperature ranging from Ts to 1500°C) (Ts: Surface temperature). Next one is equiaxed grain region (at 1500°C to 1800°C) having 97% of theoretical density and the next one is columnar region (at temperature greater than 1800°C) having 99% of theoretical density.

3.5.2. Restructuring

The fuel restructuring involves two types of grain growth. Above ~1500°C, the grains grow uniformly to produce larger equiaxed grains. The growing grains sweep up the sinter pores and trap them in boundaries. Above ~1800°C, directional grain growth begins, leading to the formation of long and narrow columnar grains that are oriented towards the hot centre of the fuel. These are believed to form by two possible mechanisms: either by the migration of the pores up the temperature gradient or by a solid state diffusion process. In the former process, it is envisioned that the fuel on the hotter side of a large pore evaporates and condenses on the cooled side, creating a transport process for the pore up the thermal gradient. The movement of the pores to the fuel results in densification of the grains and the formation of a central hole or “void”. The grain densification causes the fuel thermal conductivity to rise a little and to cause the centre temperature to drop a little.

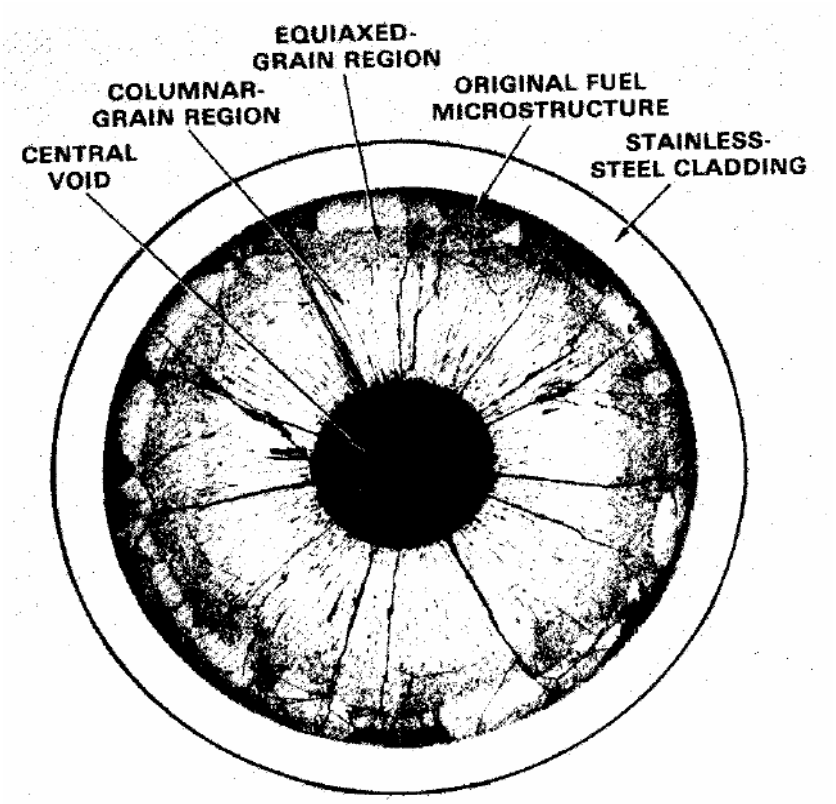

Fig.3.6 : Cross section of a typical irradiated mixed oxide fuel pin

Fig.3.6 shows the cross section of the mixed-oxide fuel pellet irradiated at a linear power of 56 kW/m to a burn-up of ~27 MWd/kg. The void in the centre of the fuel element is clearly visible, as well as the very long grains associated with the columnar region and the larger grains of the equiaxed region. Outside the equiaxed grain region and adjacent to the cladding is an annulus of fuel with the original microstructure. The temperatures in this region are too low to cause any observable restructuring of the fuel material. The large black traces extending from the central void all the way to the cladding are cracks that probably developed during cooling down from the operating temperature. These cracks were probably not part of the fuel structure during most of its lifetime.

Since restructuring patterns are directly dependent upon temperature and temperature gradients, it is expected that the differing axial temperature distributions in an fast reactor pin would result in a corresponding axial variation in fuel microstructure. It can take as little as 24 hours at power for the restructuring to occur. Thereafter more gradual changes occur, which are more related to the irradiation processes.

Implications of restructuring

1. Micro structural differences in the fuel affect the fission gas retention pattern. Tracks left by the pore migration within the columnar region allow fission gas to be easily vented to the central void region.

2. Due to formation of central void, the centreline temperature of the fuel comes down which is shown in figure given below.

3. The thermal conductivity of fuel is increased due to movement of pores to the central void, which also reduces the fuel temperature.

Fig. 3.7 shows the temperature distribution in a MOX fuel pin before and after restructuring.

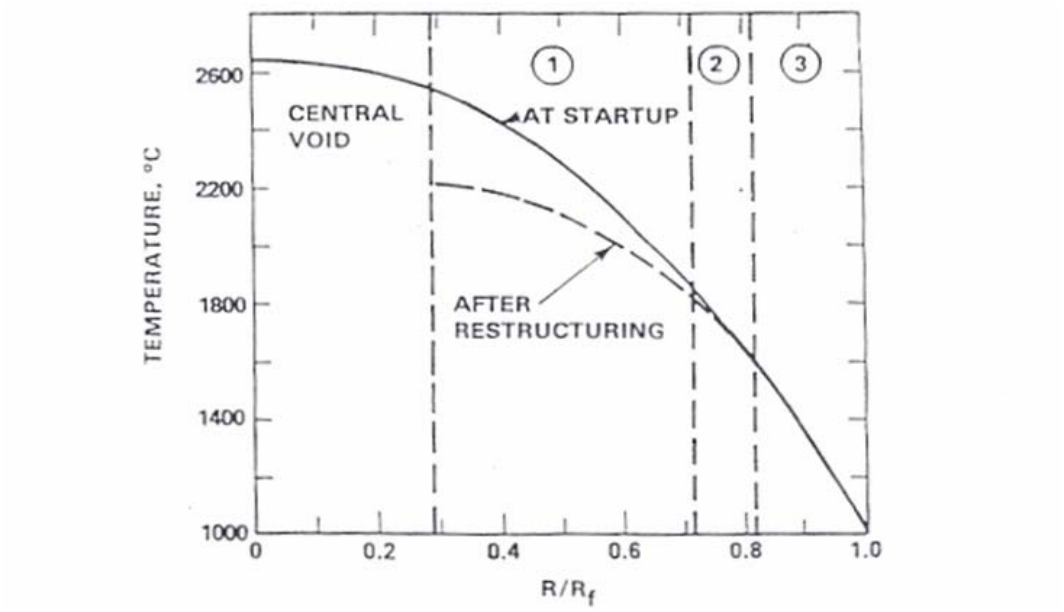

Fig. 3.7 : Temperature distribution in a MOX fuel pin before and after restructuring

3.5.3. Heat transfer in the fuel-clad gap

The computation of the temperature profile across the fuel pin is essential to study the thermal performance of the fuel pins. The drop from the fuel centre to the coolant can be identified into different zones which are fuel, fuel-clad gap, clad and the coolant film. The drop in the fuel to clad gap dictates to a large extent the maximum linear power achievable. Most experimental evidence of the irradiated fuel pins reveal that the hot gap closes after a short duration from the start up of the reactor. This is due to the fuel swelling, cracking and differential thermal expansions of the fuel and the clad. So the gap is dynamic which varies and depends on other characteristics of the fuel and the clad material. Temperature drop across the gap is given by

$$\Delta T_{Gap} = \frac{\chi}{\pi d_m h_g}$$

Where,
χ is Linear heat rating
h_g is gap conductance
d_m is mean diameter of the gap

Heat transfer can occur in the gap by conduction, convection and radiation. But the radiation and convections are negligible compared to the conduction component of the heat transfer so can be neglected. The temperature profile in the gap is shown in Fig. 3.8. The gap conductance plays a significant role in estimating the centerline temperature of the fuel pellet. To find out the gap conductance, various models are available in the literature for open and close gap shown in Fig. 3.9.

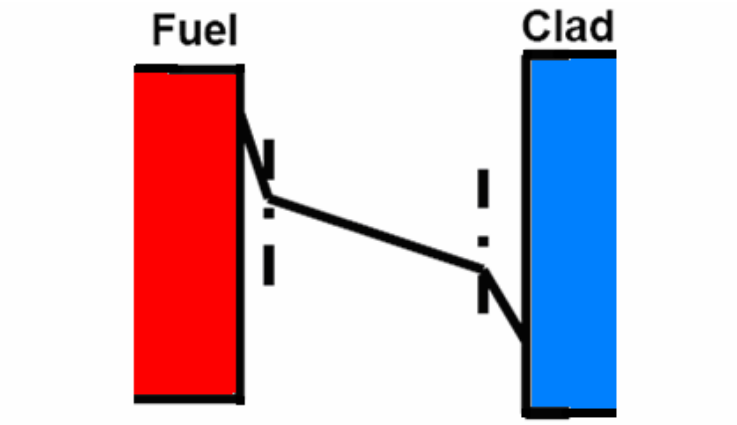

Fig. 3.8 : Temperature profile in gas

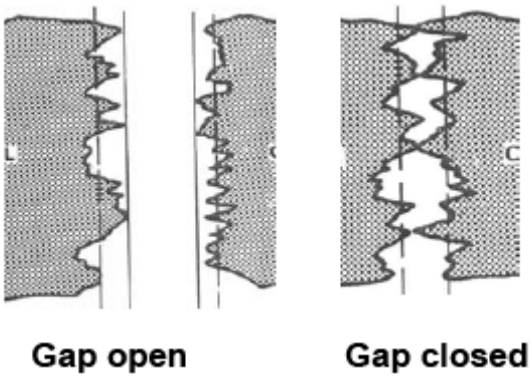

Fig. 3.9 : Types of Gap

For large open gaps, the gap conductivity is predominantly dominated by the conductivity of the gas and thus the gap conductance is given by :

$$h_g = \frac{k}{G}$$

Where,
k = Thermal conductivity of the gas and G = Open gap

But in case of smaller open gaps, the surface roughness of the fuel and clad considerably affects the temperature drop as shown in Fig 3.9. In addition to that due to the boundary layer at the surface, the thermal gradients are much steeper which can be considered by virtual jump distances which makes the drop as linear which are explained in Fig. 3.10.

$$h_g = \frac{k}{G + (\delta_f + \delta_c) + (g_f + g_c)}$$

Where,

δ_f , δ_c = Surface roughness of fuel and clad respectively

g_f , g_c = Jump distance of fuel and clad respectively

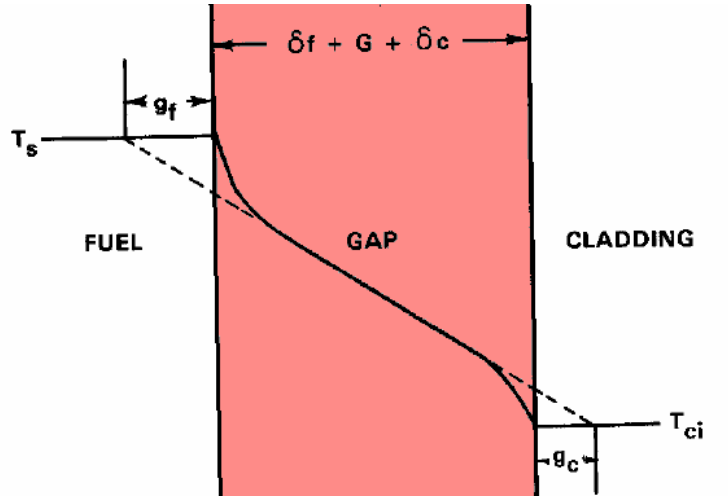

Fig. 3.10 : Open gap, jump distance parameters

In the case of closed gap, additionally contact pressure comes in to picture which enhances the gap conductance. If P_{fc} is the contact pressure and δ is the effective roughness as shown in Fig. 3.11, the gap conductivity is given by

$$h_g = \frac{Ck_s P_{fc}}{H\sqrt{\delta}} + \frac{k}{(\delta_f + \delta_c) + (g_f + g_c)}$$

Where,
C= Empirical constant
k_s = effective conductivity of surface materials
H = Meyers Hardness of softer material
δ = effective roughness

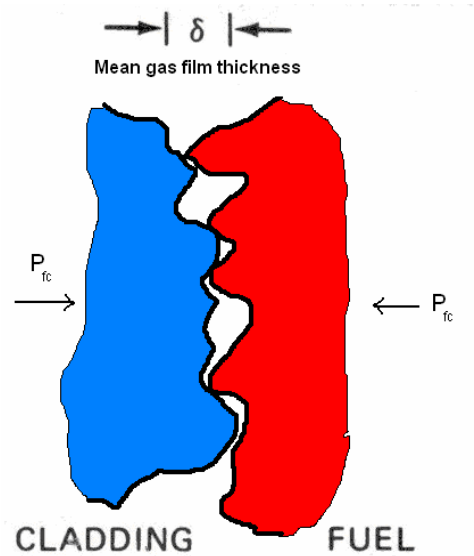

Fig. 3.11 : Closed gap with contact pressure

3.5.4. Temperature drop in the clad

The heat flux passing through the clad may be expressed as,

$$q = -K_c \frac{dT}{dr}$$

q $\rightarrow$ heat flux (W/m^2)

K_c $\rightarrow$ Thermal conductivity of cladding W/mK

This is expressed in terms of linear power.

$$\therefore \chi = -K_c \, 2\pi r \, \frac{dT}{dr}$$

K_c can be assumed constant through the clad thickness.

$$\Delta T = T_{ci} - T_{co} = \frac{\chi}{2\pi K_c} \quad ln \frac{R_{co}}{R_{ci}}$$

3.5.5. Temperature drop in the film (clad to coolant)

The heat transfer from the clad OD to the bulk coolant is expressed as

$$q = h\left(T_{co} - T_b\right) = \frac{\chi}{2\pi R_{co}}$$

Where,

h - heat transfer coefficient (W/m^{2}K)

T_{co} - Outer cladding temperature

T_b - Bulk coolant temperature

3.5.5.1 Sodium Heat Transfer coefficient, h

Fast reactor needs a coolant with a high heat transfer coefficient in order to exploit the advantage of a small fuel pin diameter. Heat transfer coefficients are higher for liquid metals than for other fluids at relatively low flow velocities and pressures; hence, liquid metals are prime candidates for use as FR coolants. The high heat transfer coefficients for liquid metals result from their high thermal conductivities compared to other fluids.

The Prandtl number, Pr, is an important dimensionless grouping of properties that influence convection heat transfer:

Prandtl No., Pr = Cp μ / K = ν / α

ν : Kinematic viscosity (μ / ρ) - related to rate of momentum transfer in a fluid.

α : Thermal diffusivity (K / ρ Cp) - related to rate of heat transfer by conduction.

For water, Pr = 1 to 10

For gases, Pr = 0.7

For liquid metals, Pr = 0.01 to 0.001

(= 0.0042 for Na at a typical mid-core temperature of 500°C)

Values of viscosity & specific heat for sodium are not appreciably different from those of water. Thermal conductivity of sodium is about a factor of 100 greater than that of water. So, for liquid metals, thickness of thermal boundary layer is substantially larger than that of hydrodynamic boundary layer. In liquid metals, molecular conduction contributes about 70% of heat transfer (In water, it is only 0.2%).

Sodium heat transfer coefficient, h for design purposes can be decided from

Nusselt No., Nu = 0.625 $Pe^{0.4}$ = hD_e/K

(Here K is conductivity of coolant & D_e is the effective hydraulic diameter)

Peclet No., Pe = Re.Pr

= (ρ v d / μ) x (μ Cp / K)

= ρ v d Cp / K

It is not a function of viscosity, μ. Various correlations are available in literature for dimensionless numbers. For example, the FFTF correlation is given below.

$$Nu = 4 + 0.33\left(\frac{P}{D}\right)^{3.8}\left(\frac{Pe}{100}\right)^{0.86} + 0.16\left(\frac{P}{D}\right)^{5} \quad \text{for } 20 \le Pe \le 1000$$

where P/D is the pitch to diameter ratio.

Hence, in liquid metal heat transfer, correlations are based on the viscosity independent Peclet number.

3.5.6. Radial temperature distribution in a fuel pin

The typical radial temperature distribution in the fuel pin is shown in Fig. 3.12 for a fast reactor fuel pin with MOX fuel. Annular concept helps in reducing the centreline temperature of the pellet for the same fuel surface temperature as shown in Fig. 3.13.

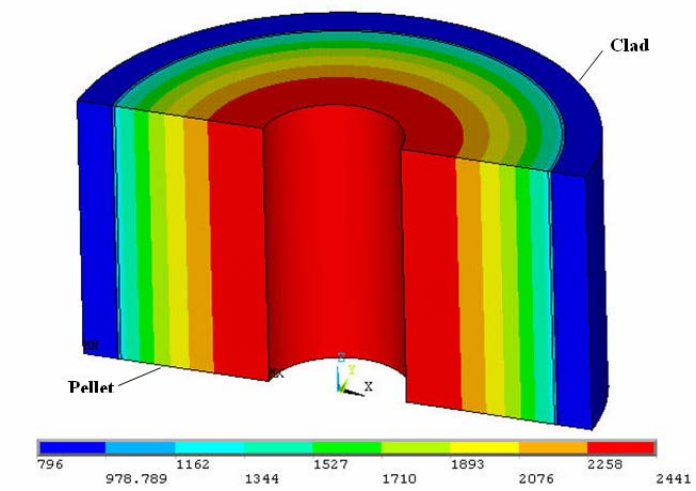

Fig. 3.12 : Radial temperature profile in a MOX fuel pin (K)

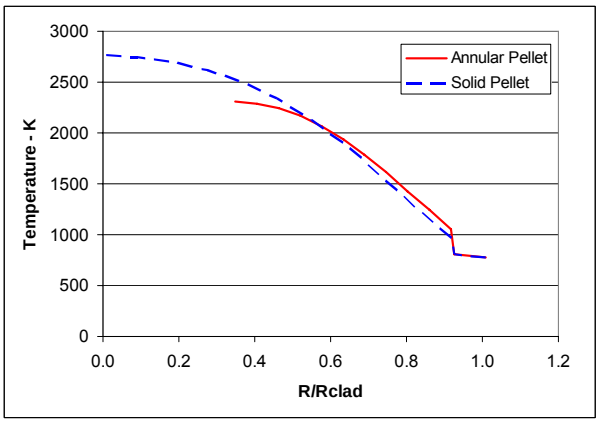

Fig. 3.13 : Typical temperature distribution in fuel pin with solid and annular pellets generating the same linear power

The annular concept is very useful in extracting the higher amount of energy from fuel. Fig. 3.14 shows the temperature profile across a pin for typical fast reactor fuel pin at different Linear Heat Ratings with constant temperature of clad outside surface.

The typical temperature distribution in case of restructured fuel element with the three-density model is shown in Fig. 3.15.

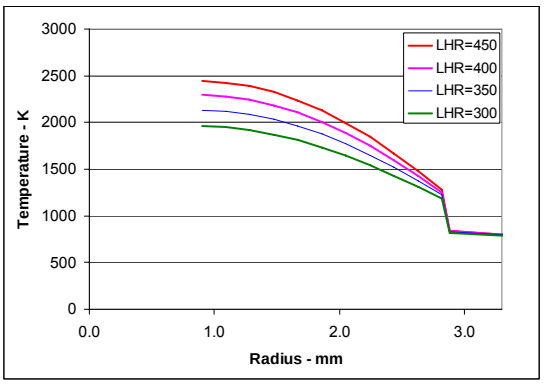

Fig. 3.14 : Radial temperature profile in case of annular pellet with different LHR

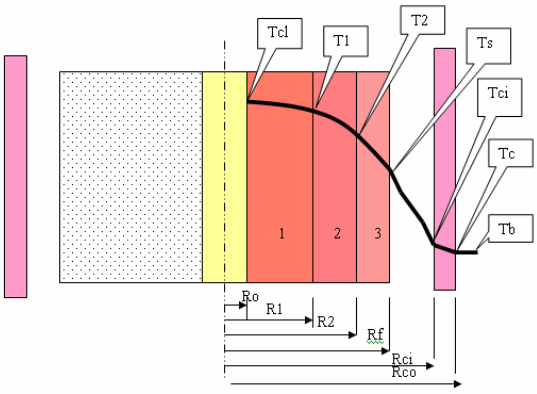

Fig. 3.15 : Temperature distribution in a fuel pin with three density model in the fuel region

3.5.7 Hot spot Analysis

The impact of uncertainties in theoretical and experimental analyses, instrumentation accuracy, manufacturing tolerances, physical properties, and correlation uncertainties must be considered in order to assure safe and reliable reactor operation. The thermal hydraulics design of a fast reactor conform to a set of design bases, or design criteria as mentioned in the beginning of this section. Many of these relate to fuel, cladding, and coolant exit temperatures under various conditions.

One fuel design criteria for FFTF and CRBRP, for example, was that no fuel melting should occur at some specified overpower; for both reactor designs this overpower was set at 115% of rated power. The maximum allowable cladding temperature must assure fuel pin integrity. Other thermal-hydraulic design bases refer to other parameters such as allowable pressure drop and coolant flow velocities.

In order to satisfy design bases, design limits must be specified which are covered in the next section. This is often done by establishing a statistical level of confidence with which selected parameters must be known. An uncertainty in a parameter, or a limiting value, is then associated with the specified level of confidence.

Uncertainties and limiting values are treated through the use of hot channel factors, or hot-spot factors. The hot channel factor, F, for a particular parameter is the ratio of the maximum value of that parameter to its nominal value. It is therefore a number greater than unity, and the decimal part (i.e., F-1) represents the fractional uncertainty in the parameter. Hot channel factors must be based on a combination of experimental data and experimentally verified analytical methods; justification of these factors is one of the most important and challenging of the reactor designer's tasks.

The hot spot analysis is to find maximum possible temperature of clad taking into account of all uncertainties. Three methods used for analysis are Deterministic method, Statistical method and Semi-statistical method.

3.5.7.1. Deterministic method

This is the oldest and most conservative method. This method is based on the assumption that all uncertainties have the most unfavourable value and occur at the same time at the same location, which is certainly very pessimistic and conservative. It virtually requires absolute certainty that the limits will not be exceeded at any location in the core.

Clad inside temperature is given by,

$$T_c = T_i + \Delta T_1 + \Delta T_2 + \Delta T_3$$

T_i = Coolant inlet temperature

ΔT_1 = temperature of coolant between point of entry of channel and point of maximum design value of Tc

ΔT_2 = film temperature drop

ΔT_3 = clad temperature drop

For each of design variables, there exists some 'worst possible value'. Tc is calculated using these values. Designer can be quite sure that nowhere else will the cladding temperature be superior to this critical temperature.

3.5.7.2. Statistical method

This is an optimistic method, since all variables that appear in calculation are not randomly distributed. Here, it is assumed that the variables follow the law of a standard statistical distribution.

3.5.7.3. Semi-statistical method

In this method, the variables that cause the hot spot temperature are separated into two principal groups, i.e., variables of statistical origin and non-statistical origin.

Exact values of the variables of non-statistical origin are not known in advance and they are not subject to random occurrence. By calculating the total hotspot factor for a certain temperature rise, the uncertainties of systematic order are treated cumulatively and the uncertainties of statistical origin are treated statistically.

3.5.7.4. Application of hotspot factors in design

The maximum fuel temperature $Tf_{\max}$ is evaluated by the following equation with the nominal values obtained in the fuel temperature analysis:

$$Tf_{\max} = T_i + F_{channel} \times \Delta T_{channel} + \sum_{i=1}^{4} F_i \times \Delta T_i$$

where T_i: Coolant inlet temperature to the core

$\Delta T_{channel}$: Hottest Channel temperature rise (taking into account of overpower)

$F_{channel}$: Channel hot spot factor

ΔT_i : Nominal temperature rise in different regions denoted by i

F_i : Overall hot spot factor for the temp drop in region i

i =1 : Film temperature rise

2 : Temperature rise in clad

3 : Gap temperature rise

4 : Temperature rise in fuel

To determine the overall hotspot factors for each component; sub factors are determined individually according to the functional relationship between the uncertainty and the temperature under consideration. These sub-factors are divided into two groups; one group occurs randomly, e.g., manufacturing tolerances and physical properties, and the other affects the entire core or large portion of it.

The random sub-factors (statistical sub-factors) fr_i are combined to give the total random sub-factor Fr_i,

$$Fr_i = 1 + \sqrt{\sum_{j=1}^{m(i)} (fr_{i,j} - 1)^2}$$

and the total systematic sub-factor Fs_i is given by combining systematic sub-factors (cumulative sub-factors) $fs_{i,k}$,

$$Fs_i = \prod_{k=1}^{n(i)} fs_{i,k}$$

where m(i) and n(i) are total number of random and systematic sub-factors, respectively.

The overall hot spot factor affecting component i is calculated by the following definition:

$$F_i = Fr_i + Fs_i - 1$$

Thus hot spot factors are applied to find the centreline temperature of fuel. Typical values of hot spot factors are:

clad: 1.3 – 1.4, , film: 2 – 2.4, channel : 1.1 – 1.3

3.6 Hydraulic design

Hydraulic design and thermal design of core have conflicting requirements. Thermal design presents the limits on clad temperature, ΔT across core and fuel centre line temperature. For the above constraints, large flow rate is favoured. But pump limitation restricts the coolant flow rate and ΔP across core. Other limiting parameters are hydraulic lifting force, cavitation, corrosion and vibration in fuel pins

To start with, minimum possible coolant requirements from thermal considerations is found out. Then, various constraints (or parameters) characterising the core hydraulics are checked whether they are within the reasonable limits.

3.6.1 Factors to be reviewed for Core Hydraulic Design

The parameters to be considered in the hydraulic design are given below. The analysis to be carried out will vary depending on the design variants and parameters adopted in a particular fuel SA design. Here, the methadology is explained for a typical design which has been used in French and Indian fast reactors. Essentially, the principles remain the same.

- Pressure drop (ΔP) across core
- Coolant flow through the core
- Coolant velocity
- Hydraulic lifting force
- Mixing studies
- Power flattening & flow zoning
- Vibration due to flow

3.6.2 Pressure Drop in Subassembly

In fast reactor primary circuit, the pressure drop through the core forms about 90% of total pressure drop. All the subassemblies in the core are fed from a common coolant inlet plenum and discharge the hotter sodium into a common outlet plenum (hot pool). Hence, pressure drop through all the subassemblies is same. The pressure drop across the core is dictated by the SA, which is receiving the maximum coolant flow. This is normally the central SA (fuel), which generates the maximum power. A typical fast reactor fuel subassembly is shown in Fig.3.16. Because the flow allocated in the peripheral SAs is less than central SAs and internal characteristics of the SA are same, it offers less pressure drop than the central SA. To equate the pressure drop, an external pressure drop device (orifice plate) is fitted in the foot of the SA. Since central SA is taken as the controlling SA for evaluating the core pressure drop, it does not have orifice plate. Criteria to limit Δp are pump availability and loading on components like core support structure and hold down mechanism. Typical value of ΔP is 70 to 80 m of Na head at 500^{o}C. This is the pressure drop through maximum rated SA as it requires maximum flow rate.

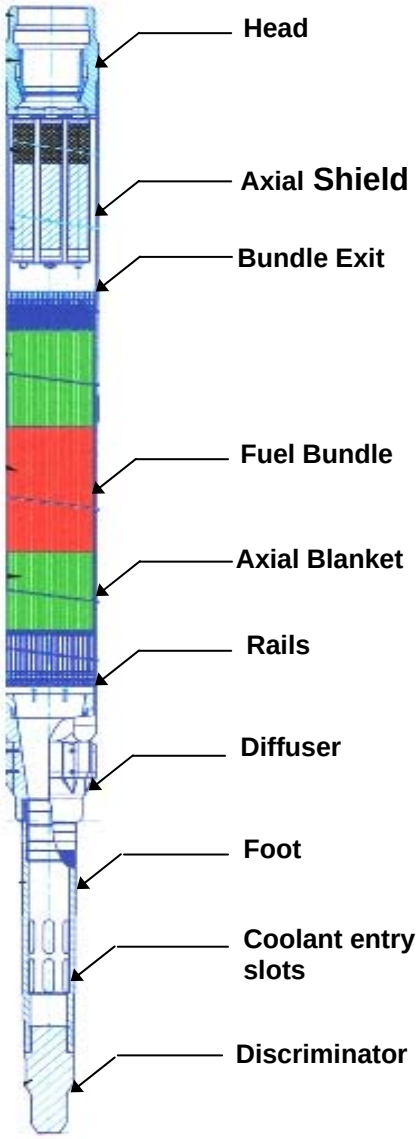

Fig 3.16: Typical Fuel SA

To evaluate the pressure drop in the maximum rated SA, it can be divided into following components:

a) Entry loss at foot
b) Frictional loss in foot
c) Loss in the transition from foot to body (bottom diffuser)

d) Loss in supporting rail for the fuel pins
e) Loss due to sudden contraction at the entry of the bundle
f) Loss along the length of bundle
g) Loss due to sudden expansion at the exit of the bundle
h) Loss in the transition from exit of bundle to the top shield
i) Frictional loss in top shield
j) Transition loss from top shield to top the head region
k) Frictional loss in head region
l) Loss due to sudden expansion at the exit of subassembly.

All the losses above mentioned except bundle loss can be dealt by conventional methods. Pressure drop in each region is estimated by empirical and standard correlations and / or verified by experiments.

3.6.2.1. Entry losses at the foot

The coolant entry to the foot of the subassembly from inlet plenum is through the holes provided in the support sleeves in the grid plate and the slots provided in the foot. Since, the slot is very near to the holes and has dimension larger than of holes, the entry losses at the foot can be taken that as the loss due to the holes in the support sleeves. The entry losses consists of :

i) Loss in holes in support sleeves

ii) Mixing of six jets in same axial location.

No empirical correlation is available in the literature for estimating the loss due to mixing of jets. It is to be arrived by experiments. Typically, it will be around 1 m of sodium.

For estimating the loss due to holes following correlation is used :

$$\Delta H = \frac{q2}{a^2 . c_e^2 . 2g} \qquad (1)$$

where q = flow rate through the hole (m^3/ s)
a = area of hole (m^2)
c_e= entrainment coefficient which is expressed by the following correlation

$$\frac{c_e}{c_o} = \cos\theta \left(\frac{A}{A^1}\right)\left(\frac{E^1}{E}\right)^{0.5} \qquad (2)$$

where,

C_O = entrainment coefficient at very high Euler numbers in which case, the jets enters normal to the stream; this coefficient can be considered as due to concentration for which a value ~ 0.58 can be taken.

$$E = \frac{v_e^2}{v_o^2} \qquad (3)$$

$$E^1 = \frac{E-1}{\left(A/A^1\right)^2} + 1 \qquad (4)$$

$$\theta = \cot^{-1}\frac{V_e}{V_o} \qquad (5)$$

The subscript e and o refers to the entry to the hole and in the foot of subassembly respectively. A refers to the area of the foot of the subassembly.

Using equations (1) through (5), loss can be estimated with an uncertainty of ± 20%. After combining the loss due to mixing of jets, the entry loss can be estimated. However, experiments are normally carried out to confirm the theoretical estimates.

3.6.2.2. Friction loss in foot, top shield and head portion

This can be estimated by well known correlation

$$\Delta H_f = f \frac{L}{D_e} \frac{V^2}{2g} \quad (6)$$

The friction factor for the smooth straight pipe can be estimated by Blassius's correlation

$$f = 0.316\ Re^{-0.25} \quad (7)$$

The losses can be estimated with an uncertainty of ±10%.

3.6.2.3. Losses due to Rail, sudden contraction at bundle entry, sudden expansion at bundle exit

The loss can be estimated by using the formula

$$\Delta H_i = K_i \frac{V_i^2}{2g} \quad (8)$$

where K_i is the loss coefficient

V_i is the average velocity in smaller section 1

The subscript i = c denotes loss due to smaller section
= e denotes loss due to expansion
= R denotes loss due to rail.

Now the values of

$$K_c = 0.5 \left(1 - \frac{A_b}{A_t}\right) \quad (9)$$

$$K_e = \left(1 - \frac{A_b}{A_t}\right)^2 \quad (10)$$

$$K_R = 0.7 \quad (11)$$

Where A_b= flow *area* of bundle
A_t= total area of the wrapper without bundle.

The rail loss and loss due to sudden contraction to the bundle entry can be found out with an uncertainty of ± 20%.

3.6.2.4. Loss along the length of the bundle

In case of fuel bundle region still studies are going on. In most of the fast reactors, wire wrap concept is used for pin separation which is compact, helps in mixing & minimizes the interaction loads. The bundle flow region is divided in to three different channels based on their shape shown in Fig. 3.17. Since all are parallel channels, the overall pressure drop in the bundle is a function of pressure drop in the centre channel because of less cross sectional area. The pressure drop in drop in individual channel is found out by following equation:

$$\Delta H_i = f_i \frac{L}{De_i} \frac{V^2}{2g} \quad (12)$$

$$f_i = \frac{C_{fi}}{Re_i^m} \qquad (13)$$

where,

ΔH_i = pressure drop in channel i
F_i = effective friction factor in the channel i
De_i = effective hydraulic diameter
Vi = average velocity in channel i
L = length of the bundle

i = 1 indicates interior sub channel
= 2 indicates wall sub channel
= 3 indicates corner sub channel

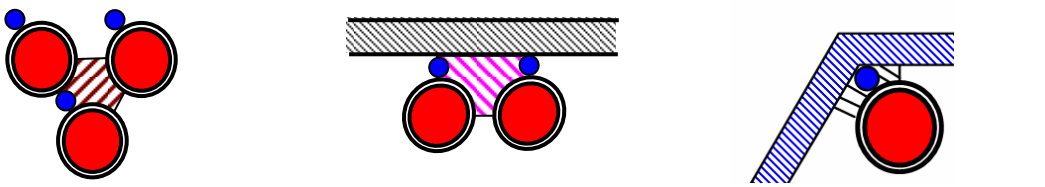

Fig.3.17 : Various sub-channels in wire wrapped fuel bundle

Various correlations are available in the literature to find out above parameters. For calculation purpose, Cheng's correlation available in literature is used as it covers a wide ranges of Reynolds number, Pitch -to-.diameter ratio and wire - wrap pitch - to - diameter ratio.

3.6.2.5. Losses in the transition from foot to body and top shield to head region

The loss can be found out from the relation

$$\Delta H_d = K_d \frac{V^2}{2g} \qquad (14)$$

The loss coefficient K_d depends on angle α and area ratio. The values of loss coefficient in the transition

(i) from foot to body, $K_{d1} = 0.13$
(ii) from top shield to head portion, $K_{d2} = 0.18$

The uncertainty involved is ± 20%

3.6.2.6. Loss in transition from body to top shield

The loss can be found out from the relation

$$\Delta H_n = K_n \frac{V^2}{2g} \qquad (15)$$

For nozzle, the loss coefficient is very small and can be taken as 0.05. The uncertainty involved is ± 20%.

3.6.2.7. Exit loss

The loss due to sudden expansion into an infinite medium can be estimated from

$$\Delta H_E = 0.5 \frac{V^2}{2g} \qquad (16)$$

and the comparison of experimental and theoretical values are shown in Fig. 3.18. The velocities at different regions in the SA are given in Table 3.2.

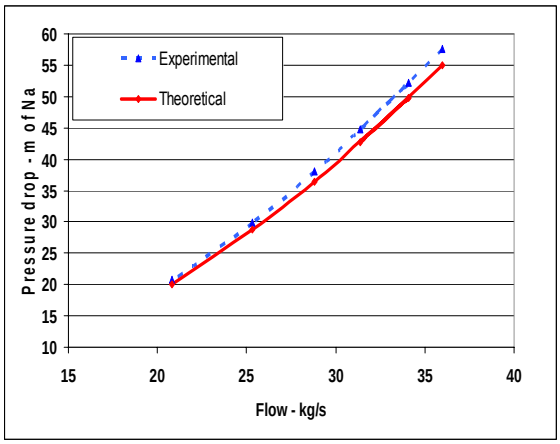

Fig. 3.18: Comparison of theoretical and experimental pressure drop in bare fuel subassembly at different flow rates

Table 3.2 : Velocity at various axial regions of SA

Si. No.	Flow path	Velocity (m/s)	
		At rated flow of 36 kg/s	At 110 % of rated flow
1	Holes in sleeves	6.6	7.2
2	Foot	15.0	16.5
3	Before Rails	3.1	3.4
4	Bundle - Entry	7.5	8.2
5	Bundle - Middle	7.6	8.4
6	Bundle - Exit	7.8	8.6
7	Top shield	8.7	9.6
8	Exit	3.7	4.0

Central Subassembly **Peripheral Subassembly**

Fig. 3.19 : Typical coolant temp distribution in central and peripheral SA

Fig.3.19 shows the typical radial coolant temperature distribution across the SA width across flats for the Sas in the core centre and a peripheral positions. Similarly, axial temperature profile is also shown in Fig. 3.20.

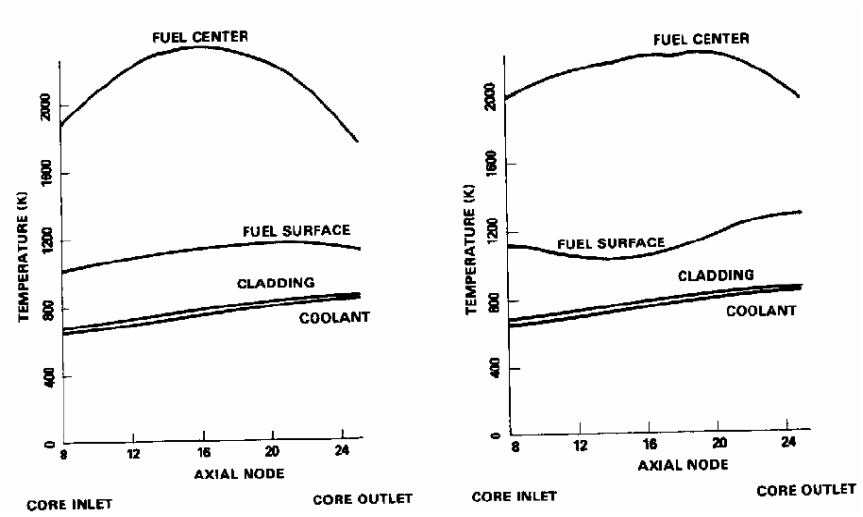

At BOL **After 65 GWd/t burnup**

Fig. 3.20 : Axial temperature profile in the FFTF fuel pin

3.6.3. Hydraulic Lifting Force

The liquid sodium as coolant flows from the primary pumps into the plenum of the grid plate, which supports the core SAs. Sodium enters the SA foot which supported on the grid plate sleeve in radial direction from the grid plate plenum passes through the fuel bundle, and extracts the heat from the pins. The flow path in the reactor assembly is shown in Fig. 3.21. The radial entry helps in hydraulic locking of the SA. The pressure of sodium at the grid plate sleeve of core SAs is very high and slowly decreases as the coolant moves out of the SA at top.

The hydraulic lift forces are developed due to the frictional drag and thrust experienced by the parts of the SA due to the flow. These forces along with buoyant force act opposite to the weight of the SA. Hence, the net downward force is lower than the actual weight of SA.

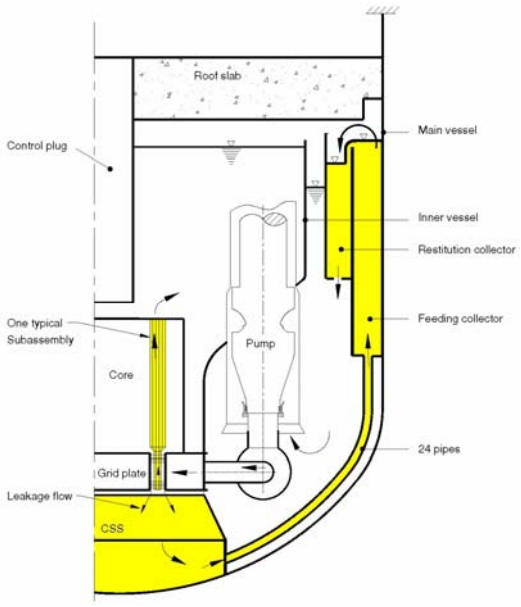

Fig. 3.21 : Primary sodium flow

The downward force consists of the weight of the SA, Pressure force on the top of the discriminator and at the diffuser. The upward force consists of Buoyancy force, lifting and drag force at orifice and at fuel or blanket bundle. For calculating the forces, the pressures at different regions are found from the total head using Bernoulli's equation 1. The total head consists of pressure head, velocity head and frictional losses occurred up to that level and head of Na column above the corresponding level.

$$\frac{P}{\rho g} + \frac{v^2}{2g} + Z + losses = Const.$$

Downward force on SA	= weight of SA + downward hydraulic pressure force
Upward force on SA	= buoyant force + upward hydraulic pressure force + drag force.
Net Downward Force	= Downward Force – Upward Force

Depending on the subassembly design, the type of forces have to be suitably accounted for. The design criteria for the hydraulic lifting of the SA would be that the net downward force acting on the SA should be more by *certain* % weight of the SA and it should not be lifted even at a flow higher than the design flow to account for over speeding of pumps. The criteria may vary between country to country. The net hydraulic hold down force on SA will be varying for different flow zones based on the coolant velocity. The net hold down force on a typical PFBR fuel SAs which weighs 2400 N is shown in Table 3.3 & Fig. 3.22

Table. 3.3 : Net downward forces on various SA of PFBR

Region	Wight of SA N	Flow Zone	100 % nominal flow			110 % nominal flow		
			Mass flow rate (kg/s)	Net Downward Force		Mass flow rate (kg/s) N	Net Downward Force	
				N	% of weight		N	% of weight
Fuel - inner	2403	1	35.83	1885	78	39.41	1844	76
		2	31.40	1926	80	34.40	1895	78
		3	28.80	1950	81	31.68	1923	80
Fuel - outer	2403	4	34.10	1899	79	37.51	1861	77
		5	28.80	1950	81	31.68	1923	80
		6	25.30	1980	82	27.83	1959	81
		7	20.82	2012	83	22.90	1998	83
Blanket	3139	8	6.03	2780	88	6.633	2779	88
		9	5.69	2780	88	6.259	2779	88
		10	4.3	2782	88	4.73	2781	88

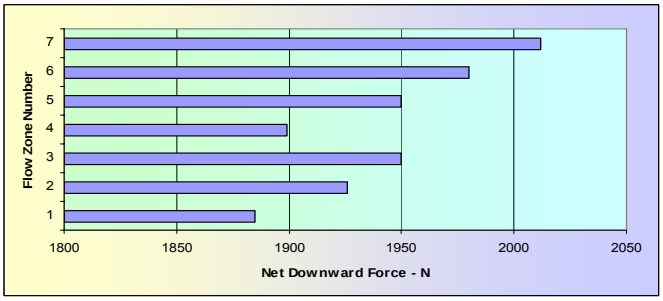

Fig. 3.22 : Hydraulic force on a typical PFBR fuel subassembly in different zones

REFERENCES

1. Nece R.E., Goldstern P.P and Black J.L – “Single-Port suction manifolds”, J. of Hydraulic Division, ASCE, HY1, 1966, PP – 43-64.
2. Cheremisinoff N.P. – “Fluid flow pocket Hand book”. Gulf Publishing Co. Book Division, Houston, 1984.
3. Cheng S.K and Todreas N.E. – “Hydrodynamic models and correlations for bare and wire wrapped hexagonal rod bundles – bundle friction factors, sub channel friction factors and mixing parameters”, Nuclear Engineering & Design, V. 92, 1986, PP – 227-251.
4. Miller Donald S. – “Internal flow systems”, V.5, BHRA Fluid Engineering Series, 1978.
5. Preliminary Safety Analysis Report of PFBR, Chapter 5.2, Core Engineering.
6. 'Design of 500 MWe Prototype Fast Breeder Reactor' - An internal document.
7. Walter, A.E. & Reynolds, A.B., 'Fast Breeder Reactors', PERGAMON Press, 1982.
8. Yevick, J.G., 'Fast Reactor Technology - Plant Design', M.I.T. Press.
9. Donald R. Olander, ‘Fundamental Aspects of Nuclear Reactor Fuel Elements’, U.S. Department of Energy, 1985
10. Idel’chik I.E., ‘Handbook of Hydraulic Resistance’, Israel Program for Scientific Translations. 1966.
11. Internal reports of IGCAR, Kalpakkam.

* * *